Low Temperature Physics/Fizika Nizkikh Temperatur, 2019, v. 45, No. 8, pp. 1045–1052

On the magnetoelectric effect in paramagnetic $NH_2(CH_3)_2Al_{1-x}Cr_x(SO_4)_2{\cdot}6H_2O$ crystals

V. Kapustianyk[1,2], N. Loboda[2], Yu. Eliyashevskyy[2], and S. Semak[2]

[1]*Scientific-Technical and Educational Center of Low-Temperature Studies, Ivan Franko National University of Lviv*
50 Dragomanova Str., Lviv 79005, Ukraine
E-mail: kapustianyk@yahoo.co.uk

[2]*Department of Physics, Ivan Franko National University of Lviv, 50 Dragomanova Str., Lviv 79005, Ukraine*

Received February 25, 2019, published online June 26, 2019

The recently reported ability to induce and tune a sign of the magnetoelectric (ME) interactions in $NH_2(CH_3)_2Al_{1-x}Cr_x(SO_4)_2{\cdot}6H_2O$ crystals as a function of Cr content is further investigated here. The ME coupling and its larger absolute value for the sample with larger Cr content agrees qualitatively with thermodynamic Landau analysis. However, quantitative estimation implies other contributions as well. The observed nontrivial magnetic field dependence of ferroelectric transition can be explained within the model that takes into account influence of the arising local deformation of the lattice on the two types of DMA group responsible respectively for the ferroelectric and antiferroelectric ordering.

Keywords: magnetoelectric interaction, paramagnetic, ferroelectric transition.

Introduction

Motivated by ever increasing miniaturization needs the magnetoelectric (ME) effects in solids are intensively studied in the last decades challenging modern solid state physics [1,2] and spin electronics [3–6]. In the latter case establishing low-power electric control over magnetic pillars would be highly beneficial for magnetic memory structures reducing power dissipation. Although large values of magnetization and electric polarization are often motivating factors for ME materials research [7–9], ferromagnetism and ferroelectricity tend to be mutually exclusive in a single phase [10] and the largest ME coupling is mostly seen in inorganic antiferromagnets at symmetry-breaking spin reorientation transitions [11]. While the number of known compounds of this type is constantly increasing the ME coupling generally occurs at very low temperatures. In that respect, the possible solution is to focus on ME coupling of higher orders that is known to be symmetry independent [12,13] and can involve elastic interactions as a common fulcrum property. In the latter case materials with low values of the Young's modulus may be advantageous due to larger pressure dependence of their physical properties. In that respect hybrid organic-inorganic structures offer an important alternative. Moreover, ME coupling in materials with magnetic ordering other than anti-ferro-ferrimagnetic becomes important. For example, a large ME effect was reported to exist in the paramagnetic $[(CH_3)_2NH_2]Mn(HCOO)_3$ [14]. Accompanied by other effective examples [15–20], this result reveals a large prospective of organic-inorganic materials [21] in the research of ME compounds and beyond [22,23].

Using the fact that electric order in the lattice is generally more fragile than a magnetic one, the ion metal substitution can be used to introduce magnetic ordering and possibly ME coupling to already known electrically polar materials. In this regard the organic-inorganic hybrid frameworks really offer a richness of possibilities [24–38]. Indeed, in our recent study [38] as the initially diamagnetic and ferroelectric crystals of $NH_2(CH_3)_2Al(SO_4)_2{\cdot}6H_2O$ (DMAAlS) known to be electrically polar below 152 K [33,34] became paramagnetic. The crystal structure of these crystals is constructed with Al cations coordinated by six water molecules (i.e., water octahedral), regular $(SO_4)^{2-}$ tetrahedral and $[NH_2(CH_3)_2]^+$ (DMA) cations, all hydrogen bonded to a three dimensional framework (Fig. 1). Thus, Al can be easily substituted with magnetic Cr resulting in $[NH_2(CH_3)_2]Al_{1-x}Cr_x(SO_4)_2{\cdot}6H_2O$ formula. For the chosen amount of Cr (x = 0.065 and 0.2) the octahedra become occupied by statistical mixtures of magnetic Cr- and nonmagnetic Al-atoms.

Upon cooling these crystals exhibit a second order phase transition at T_c = 152 K from paraelectric but ferroelastic ($T > T_c$) to ferroelectric ($T < T_c$) phases. The phase transi-

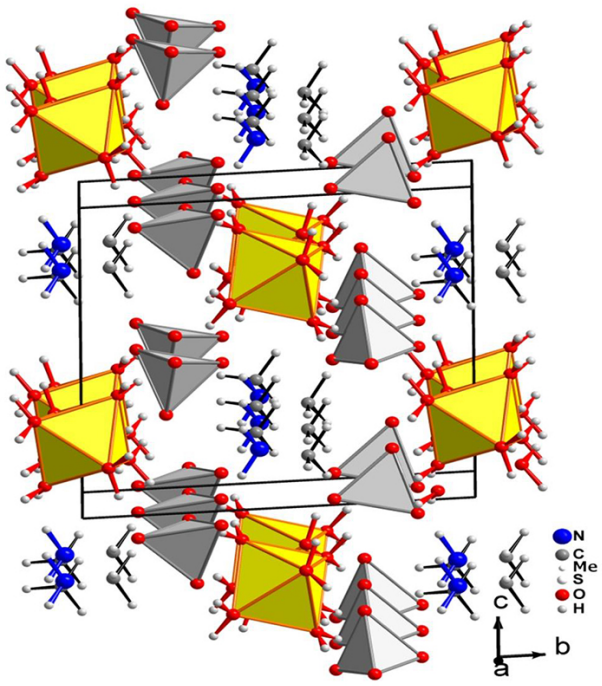

Fig. 1. (Color online) Crystal structure of non-centrosymmetric monoclinic $DMAAl_{1-x}Cr_xS$ at 135 K. The Me-ions are in the centers of yellow $[H_2O]_6$-octahedra. In the crystal structures of $[NH_2(CH_3)_2]Al_{1-x}Cr_x(SO_4)_2{\cdot}6H_2O$ with x = 0.2 and 0.065 octahedra are occupied by statistical mixtures of magnetic Cr- and weakly magnetic Al-atoms. $[SO_4]^{2-}$-tetrahedra are depicted in grey color.

tion is of the order-disorder type with a symmetry change $2/m \rightarrow m$. It is connected with ordering of the polar DMA cations which execute hindered rotations around their C–C direction in the paraelectric phase and order only in the spatio-temporal average in the ferroelectric phase [35]. Metal ion isomorphous substitution in the above mentioned family of compounds can be an additional degree of freedom in the composition-property engineering [36,37]. Besides creation of the paramagnetic with Cr increment [38] the large ME coupling was successfully generated [38]. Moreover, the possibility to tune its sign changing the Cr content was demonstrated. Unfortunately, a brief format of the paper in the corresponding journal did not allow describing the above mentioned effect in detail. Here we report the detailed analysis of electric, magnetic properties and ME interactions in the $[NH_2(CH_3)_2]Al_{1-x}Cr_x(SO_4)_2{\cdot}6H_2O$ (x = 0.065; 0.20) crystals including the phenomenological approach for evaluation of the ME coupling strength.

Experimental

Single crystals of $[NH_2(CH_3)_2]Al_{1-x}Cr_x(SO_4)_2{\cdot}6H_2O$ ($DMAAl_{1-x}Cr_xS$) were grown from an aqueous solution containing the metal sulphates in a stoichiometric ratio and dimethylammonium sulfate at a constant temperature of 303 K by slow evaporation method. The molar ratio of Al^{3+}: Cr^{3+} in the solution was equal to 1: 0.065 and 1: 0.2, respectively. This ratio in the samples was controlled by SEM using a REMMA-102–02 (SELMI, Ukraine) scanning electron microscope. Quantitative electron probe microanalysis (EPMA) of the phases was carried out using an energy-dispersive x-ray (EDX) analyzer with the pure elements as standards (the acceleration voltage was 20 kV; *K*- and *L*-lines were used). The obtained values of Al^{3+}: Cr^{3+} molar ratio were found to be 0.065±0.006 and 0.2 ± 0.02 (for a single domain sample) and correspond to those in the reacting solution.

The measurements of the real part of dielectric permittivity and conductivity were carried out using the traditional method of capacitance measurement. The capacitance was measured using an automated setup based on a LCR-meter HIOKI 3522–50 LCF HiTester. The spontaneous polarization was measured using Keithley 6517A electrometer. The magnetic susceptibility was measured using a commercial magnetometer Quantum Design MPMS-3 in the temperature range of 1.6–300 K and magnetic fields up to $\mu_0 H$ = 7 T. For both polarization and magnetic measurements electric and magnetic fields were applied perpendicular to the crystallographic plane in the monoclinic crystal structure (parallel to the polar axis).

Results and discussion

The temperature dependences of the dielectric permittivity ε' for $DMAAl_{1-x}Cr_xS$ (x = 0; 0.065; 0.2) crystals obtained at comparatively low frequencies of measuring field (Fig. 2(a)) can be used for the precise determination of the phase transition temperatures in the samples with different chromium concentration. Indeed, dielectric permittivity manifests sharp anomalies at T_c temperature characteristic of the proper ferroelectric phase transition for all investigated $DMAAl_{1-x}Cr_xS$ crystals. The temperatures of the phase transition for the samples with a different chromium concentration are presented in Table 1.

Table 1. Curie temperatures for $DMAAl_{1-x}Cr_xS$ crystals

	DMAAlS	$DMAAl_{0.935}Cr_{0.065}S$	$DMAAl_{0.8}Cr_{0.2}S$
T_c, K	152.5	154.9	153.1

Similarly to the initial compound the value of the dielectric permittivity for $DMAAl_{0.8}Cr_{0.2}S$ samples is almost three orders of magnitude larger for an AC electric field applied along the *a* axis confirming the spontaneous polarization direction (Fig. 2(a)). The pyroelectric measurements for $DMAAl_{0.8}Cr_{0.2}S$ confirm and compliment the electrically polar character of the transition. A distinct clear peak in the current is observed at the same temperature (Fig. 2(b)) where both dielectric permittivity and thermal expansion also show anomalies. A dc electric field of 7.9 kV/m applied during cooling reveals peaks in the pyroelectric currents for both samples and demonstrates Cr dependent T_c evolution.

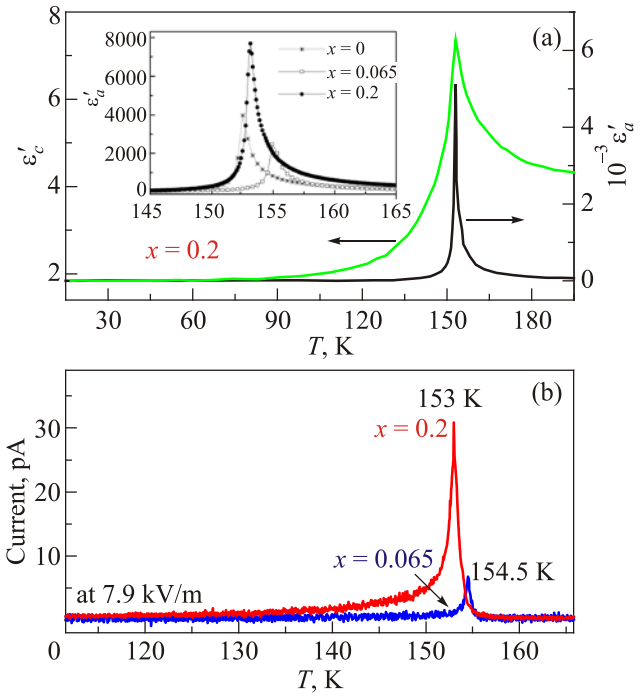

Fig. 2. (Color online) Temperature dependences of the structurally correlated electric properties. (a) The real part of the dielectric permittivity ε'_a and ε'_c for $DMAAl_{0.8}Cr_{0.2}S$ crystals measured at 5 kHz. Inset: Temperature dependences of the real part of the dielectric permittivity ε'_a of $DMAAl_{1-x}Cr_xS$ crystals with different concentration of chromium at 100 kHz. (b) Pyroelectric currents for samples with $x = 0.2$ and 0.065 Cr content.

The phase transition temperature T_c in the sample with $x = 0.065$ was shifted toward higher temperatures in comparison with the pure DMAAlS by 2.4 K. Otherwise, increase of chromium concentration to $x = 0.2$ leads to the shift of this temperature less pronounced. The temperature of phase transition in $DMAAl_{0.8}Cr_{0.2}S$ is very close to those for the initial crystal.

The temperature dependences of the dielectric properties for both investigated crystals fairly well correlate with the data of previous investigations [37] and obey the Curie–Weiss law both in the paraelectric and ferroelectric phases in the vicinity of the ferroelectric phase transition. Together with the data of DSC study [37] this clearly confirms a second order of the phase transition. No other anomalies were observed in the pyrocurrent temperature dependences at cooling of both samples down to 1.6 K. Therefore, one can conclude that the ferroelectric phase exists in $DMAAl_{1-x}Cr_xS$ crystals in the temperature range from T_c down to 1.6 K. This conclusion is also confirmed by the temperature dependences of the electric polarization (Fig. 3(a)) measured after ferroelectric saturation occurring above 250 kV/m [39]. It is necessary to note that both parameters — the temperature of phase transition and spontaneous polarization — manifest a nonlinear dependence on chromium content and explanation of this fact is not straightforward.

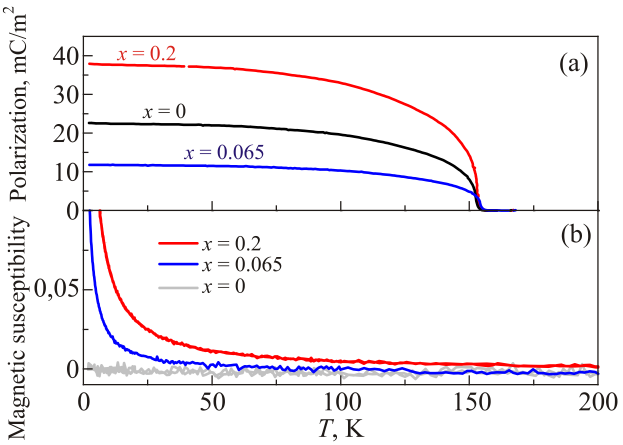

Fig. 3. (Color online) Temperature dependences of magnetic and electric properties. (a) Electric polarization. (b) Magnetic susceptibilities for $DMAAl_{1-x}Cr_xS$ crystals with different Cr content.

The temperature dependences of magnetic susceptibilities of $DMAAl_{1-x}Cr_xS$ complexes are depicted in the Fig. 3(b). The magnetic parameters are determined via CW fit of magnetic susceptibility (Table 2). The pure complex without Cr ($x = 0$) is diamagnetic in the whole studied temperature range with residual susceptibility χ_0 given in Table 2.

Table 2. Magnetic parameters for $DMAAl_{1-x}Cr_xS$ complexes

Cr-content, x	χ_0 (10^{-4} emu·mol^{-1})	μ_{eff} (μ_B)
0	–2.26(7)	
0.06	–2.40(5)	1.47(1)
0.2	–2.49(8)	1.91(1)

Isomorphous substitution of Al with Cr leads to the appearance of a paramagnetic fraction below 100 K for $x = 0.065$ and to a paramagnetic behavior and, thus positive, $\chi(T)$ for $x = 0.2$ (Fig. 3(b)). Both these susceptibilities fit excellently to modified Curie–Weiss (CW) law ($\chi = C/T + \chi_0$) in the temperature range 50–300 K (Fig. 3(b)). As one can see from Table 2, the χ_0 values obtained from the fit agree well with those of initial DMAAlS crystal. This confirms that Cr-atoms are embedded into a diamagnetic matrix. Effective magnetic moments μ_{eff} deduced from the fit depend on the chromium content, indicating noticeable Cr–Cr interactions in the studied compounds. As it is known, Cr^{3+} usually forms octahedral complexes [40]. The Al^{3+} ions (in this crystallographic position the Cr substitution is expected) center octahedral voids in the studied structures (Fig. 1). Both these facts hint toward +3 oxidation state for Cr (i.e., $3d^3$ electronic configuration) and thus, a low spin type of complex in agreement with earlier studies [36]. Interestingly, no anomalies are seen in the magnetic susceptibilities at ferroelectric T_c as it would be expected from [14]. However, careful examination of the derivatives $d\chi/dT$ performed in [38] revealed a clear deviation from linearity near T_c for the $DMAAl_{1-x}Cr_xS$ crystals

and temperature independent linear behavior for the initial sample. Even more, the magnetic susceptibility derivative for the crystal with x = 0.065 showed an upturn towards low temperatures while for x = 0.2 an upturn occured towards high temperatures [38].

Such a different behavior correlates well with the different magnetic field dependence of the pyroelectric current magnitude and its peak temperature position for both samples (Fig. 4). With increasing of magnetic field the intensity of the peak in pyrocurrent increases and shifts towards higher temperatures for the compound with x = = 0.065, while for x = 0.2 the opposite effects are observed. The temperature dependences of the spontaneous polarization (Fig. 5) calculated on the basis of the dependences shown in Fig. 4 also manifest considerable dependence on the applied magnetic field. The latter suppresses the polarization for the sample with a lower content of chromium and enlarges it for the crystal with x = 0.2. One can conclude that the applied magnetic field causes the shift of the phase transition point to the higher temperatures for the sample with x = 0.065 and in the opposite direction for the case x = 0.2. The ME coupling coefficient α_{ME} in the units of [s/m] is defined here as:

$$\alpha_{ME} = \frac{1}{\Delta H}\int (I_{H=0} - I_H)\,dt\,, \qquad (1)$$

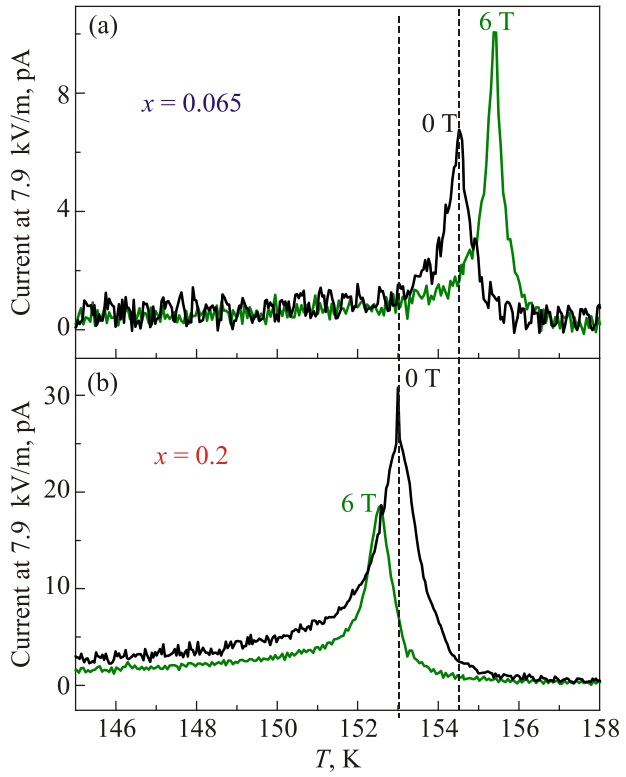

Fig. 4. (Color online) Magnetic field influence on the pyroelectricity. (a) The sample with the Cr content of x = 0.065; (b) The sample with the Cr content of x = 0.2. An opposite behavior in both magnitude and temperature position of the pyroelectric peak is observed.

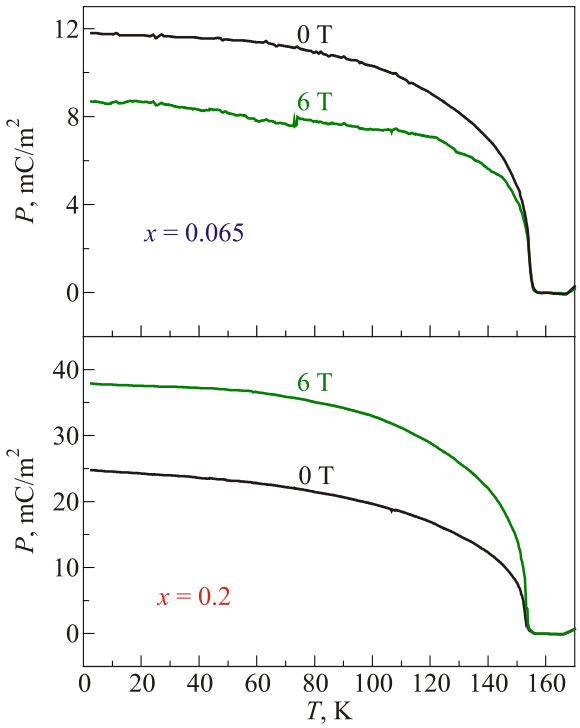

Fig. 5. (Color online) Temperature dependences of the spontaneous polarization calculated on the basis of the dependences depicted in Fig. 4.

where I is the pyroelectric current density and H is the magnetic field applied ($\mu_0 H$ = 6 T) during the measurements (Fig. 6). As one can see from the ME coupling coefficient presented in Fig. 6, the effect of coupling is stronger for the crystal with Cr content x = 0.2. As expected the absolute value of α_{ME} decreases monotonically till the FE Curie temperature is reached.

However, both crystals also show a discontinuity in ME coupling near T_c (inset to Fig. 6) implying the existence of a small coupling even in the paraelectric and paramagnetic region. The fact that the ME coupling coefficient changes

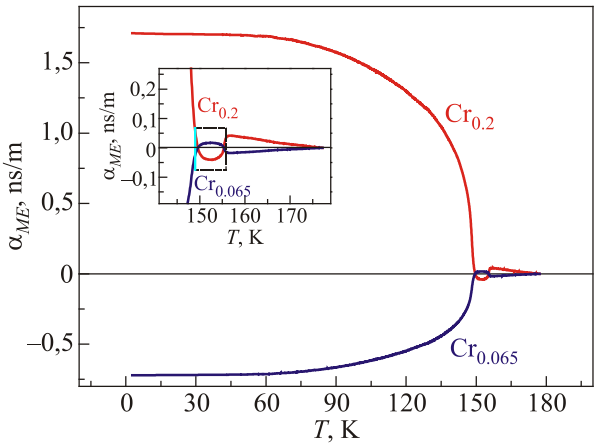

Fig. 6. (Color online) Temperature dependence of the ME coupling coefficients for parallel orientation of magnetic field and spontaneous polarization. Inset shows a zoomed region near T_c.

its sign as a function of Cr content as well as the large level of the coupling itself points towards the possibility to tune the ME response in such compounds. On the other hand, such a nontrivial behavior of the ME response demands a more detailed consideration.

The magnetoelectric effect in a single-phase crystal is traditionally described [41,42] in Landau theory by writing the free energy F of the system in terms of an applied magnetic field H whose i-th component is denoted H_i, and an applied electric field E whose i-th component is denoted E_i. Note that this convention is unambiguous in free space, but that E_i within a material encodes the resultant field that a test particle would experience. In the beginning let us consider a non-ferroic phase in respect to the magnetic or ferroelectric type of ordering, where both the temperature-dependent electrical polarization $P_i(T)$ ($\mu C{\cdot}cm^{-2}$) and the magnetization $M_i(T)$ (μ_B per formula unit, where μ_B is the Bohr magneton) are zero in the absence of applied fields and there is no hysteresis. It may be represented as an infinite and homogeneous medium by writing F under the Einstein summation convention in SI units as [41]:

$$-F(E,H)=\frac{1}{2}\varepsilon_0\varepsilon_{ij}E_iE_j+\frac{1}{2}\mu_0\mu_{ij}H_iH_j+\alpha_{ij}E_iH_j+$$
$$+\frac{\beta_{ijk}}{2}E_iH_jH_k+\frac{\gamma_{ijk}}{2}H_iE_jE_k+\ldots. \qquad (2)$$

The first term on the right hand side describes the contribution resulting from the electrical response to an electric field, where the permittivity of free space is denoted ε_0, and the relative permittivity $\varepsilon_{ij}(T)$ is a second-rank tensor that is typically independent of E_i in a non-ferroic phase. The second term is the magnetic equivalent of the first term, where $\mu_{ij}(T)$ is the relative permeability and μ_0 is the permeability of free space. The third term describes linear magnetoelectric coupling via $\alpha_{ij}(T)$; the third-rank tensors $\beta_{ijk}(T)$ and $\gamma_{ijk}(T)$ represent higher-order (quadratic) magnetoelectric coefficients.

In the present scheme, all magnetoelectric coefficients incorporate the field independent material response functions $\varepsilon_{ij}(T)$ and $\mu_{ij}(T)$. The magnetoelectric effects can then easily be established in the form $P_i(H_j)$ or $M_i(E_j)$. The former is obtained by differentiating F with respect to E_i, and then setting $E_i = 0$. A complementary operation involving H_i establishes the latter. One obtains:

$$P_i=\alpha_{ij}H_j+\frac{\beta_{ijk}}{2}H_jH_k+\ldots \qquad (3)$$

and

$$\mu_0M_i=\alpha_{ij}E_j+\frac{\gamma_{ijk}}{2}E_jE_k+\ldots. \qquad (4)$$

In the ferroic phases, the above analysis is less rigorous because $\varepsilon_{ij}(T)$ and $\mu_{ij}(T)$ display field hysteresis. Moreover, ferroics are better parameterized in terms of resultant rather than applied fields [43]. This is because it is then possible to account for the potentially significant depolarizing/demagnetizing factors in finite media, and also because the coupling constants would then be functions of temperature alone, as in standard Landau theory. In practice, resultant electric and magnetic fields may sometimes be approximated [44] by the polarization and magnetization respectively.

A multiferroic that is ferromagnetic and ferroelectric is liable to display large linear magnetoelectric effects. This follows because ferroelectric and ferromagnetic materials often (but not always) possess a large permittivity and permeability respectively, and α_{ij} is bounded by the geometric mean of the diagonalized tensors ε_{ii} and μ_{jj} such that [44]:

$$\alpha_{ij}^2\le\varepsilon_0\mu_0\varepsilon_{ii}\mu_{jj}. \qquad (5)$$

Equation (5) is obtained from Eq. (2) by forcing the sum of the first three terms to be greater than zero, that is, ignoring higher-order coupling terms. It represents a stability condition on ε_{ij} and μ_{ij}, but if the coupling becomes so strong that it drives a phase transition to a more stable state, then α_{ij}, ε_{ij} and μ_{ij} take on new values in the new phase. Note that a large ε_{ij} is not a prerequisite for a material to be ferroelectric (or *vice versa*); and similarly ferromagnets do not necessarily possess large μ_{ij} [41].

Investigated $DMAAl_{1-x}Cr_xS$ crystals undergo the phase transition into the ferroelectric phase at T_c and within this phase they hardly would be described by relations (2)–(5) taking into account the reasons mentioned above. On the other hand, one can use such an approach for description of the narrow temperature range in vicinity of T_c. Indeed, just below this point the crystal loses the centre of inversion, although the spontaneous polarization stays very small and it is possible to neglect its contribution into free energy (2). In this special case we could also neglect the term responsible for the piezoelectric interaction in the relation (2) although it would be important at lower temperatures, when the spontaneous polarization increases considerably. Under such cautions one can use the estimation (5) for analysis of the temperature dependence of the magnetoelectric coefficients. First of all this concerns the narrow diapason between 150 and 155 K (shown by the dashed rectangle in Fig. 6) which is characterized by change of ME coefficient sign on its boundaries. We took the maximal values of dielectric permittivity at T_c for calculation of the product in the right side of the inequality (5). Moreover, we chose the values of this parameter measured at 1 kHz, when the contribution of the fundamental dielectric dispersion as well as the dispersion caused by domain dynamics is negligible. These values of the dielectric permittivity were drawn from its temperature-frequency dependences and corresponding Cole–Cole diagrams [37,45]. They would be considered under certain conditions as the constants for the considered solid solutions. The obtained data of calculations according to the inequality (5) are presented in Table 3. One can con-

Table 3. Parameters of ME effect for $DMAAl_{1-x}Cr_xS$ complexes

Parameters	$DMAAl_{0.935}Cr_{0.065}S$	$DMAAl_{0.8}Cr_{0.2}S$
T, K	155.2	153.1
ε	2508	10922
μ	1	1.000313
$\varepsilon\mu\varepsilon_0\mu_0$	$2.790\cdot10^{-5}$ ns^2/m^2	$1.215\cdot10^{-4}$ ns^2/m^2
α^2_{ME}	$1.289\cdot10^{-5}$ ns^2/m^2	$15.88\cdot10^{-4}$ ns^2/m^2

clude that for $DMAAl_{0.935}Cr_{0.065}S$ the above mentioned inequality is fulfilled confirming the proposed approach.

For $DMAAl_{0.8}Cr_{0.2}S$ the estimation (5) does not look valid but it is clear on the qualitative level that increase of chromium concentration leads to considerable increase of ME coupling coefficient first of all due to a much higher peak value of the dielectric permittivity. Above the phase transition (T > 155 K) the linear ME effect is prohibited by the center of inversion, although one can note that the experimentally measured α_{ME} coefficient stays nonzero even a little above the Curie point. Such a behavior as well as nonfulfilment of the inequality (5) are connected with the fact that our crystals hardly would be considered as a stress-free medium. Indeed, the isomorphous substitution of the metal ion is followed by arising of the local lattice deformations and their contribution cannot be neglected in free energy (2) especially in the case of $DMAAl_{0.8}Cr_{0.2}S$. The observed considerable increase of the ME coefficient absolute value for both samples below T_c is connected with a considerable increase of the spontaneous polarization and analysis cannot be so straightforward.

The nontrivial dependence of the spontaneous polarization and Curie temperature on the chromium content as well as ME properties of the considered material demand more detailed consideration. Moreover, the performed analysis testifies that the above mentioned phenomena are closely connected.

ME properties can be tentatively explained by the two-fold effect. Firstly, the introduction of larger and magnetic Cr ($R_{i\mathrm{Cr}}$ = 0.6115 Å; $R_{i\mathrm{Al}}$ = 0.535 Å) into the lattice of initial DMAAlS crystal generates strains and secondly, makes the compound more sensitive to magnetic field. The magnetoelectric coupling here can arise via stress mediated contribution.

All above experimental results support the existence of certain coupling between magnetism and ferroeletricity in the paramagnetic state of $DMAAl_{1-x}Cr_xS$ crystals. The ME coupling in the paramagnetic state is unusual and there have been only very limited reports so far. The first example was reported by Hou and Bloembergen in 1964 in a piezoelectric paramagnetic crystal of $NiSO_4\cdot6H_2O$ [46]. They termed this kind of paramagnetic magnetoelectric coupling as paramagnetoelectric (PME) effects and proposed that it may appear in other piezoelectric paramagnetic crystal where the PME effect at low temperature is dominated by the variation of crystal field splitting D with electric field. The magnetic field influence on the electric polarization was also observed in the ferroelectric-ferroelastic paramagnetic phase of rare-earth molybdates such as $Tb_2(MoO_4)_3$ and $Gd_2(MoO_4)_3$ [47]. The authors ascribed this ME effect to the magnetostriction associated with Tb^{3+} and Gd^{3+} ions along with the piezoelectric effect of the ferroelectric substance.

Similarly, the ME effect in the so-called metal-organic frameworks (MOF) could be also related to the magnetostriction (magnetoelastic) effect. Situation with ME coupling in $DMAAl_{1-x}Cr_xS$ crystals looks very similar to those in $[(CH_3)_2NH_2]Mn(HCOO)_3$ that also would be related to MOFs [14]. The ferroelectricity in this MOF is associated with hydrogen bond ordering [14]. In the high temperature paraelectric phase, the DMA cations in the cavities are dynamically disordered with nitrogen distributed over three equivalent positions, because the hydrogen bonding between the hydrogen atoms of the NH_2 group and oxygen atoms from the formate frame-work is disordered. Below 185 K, the ordering of nitrogen atoms due to the hydrogen bond ordering of the DMA cations leads to a lowering in symmetry. As a consequence, a structural transition from the rhombohedral to monoclinic symmetry and *Cc* space group (*Cc* belongs to one of the 10 polar point groups required for ferroelectricity) is accompanying with the hydrogen bond ordering and the ferroelectric phase transition. The magnetic susceptibility and ESR data suggested that the monoclinic crystalline structure favors the short-range superexchange interaction between Mn^{2+} ions than the rhombohedral structure, possibly due to the modification in the Mn–Mn distance and angle.

The correlation between exchange interaction and lattice structure is known as the magnetostriction or magnetoelastic effect. Especially, a recent study by Thomson *et al.* using resonant ultrasound spectroscopy reveals that there is certain magnetoelastic coupling in the MOF family [48].

It is worth to note that the phase transition in the initial DMAAlS and $DMAAl_{1-x}Cr_xS$ crystals with a symmetry change $2/m \rightarrow m$ is connected with ordering of the polar DMA cations [35]. All DMA cations are hydrogen bonded to a three dimensional framework (Fig. 1). Therefore, ordering of DMA cations is connected with hydrogen bond ordering. According to the data of [49] DMA groups in DMAAlS belong to two different sublattices (an elementary cell consists of two translationally nonequivalent groups). The orientation of DMA groups was characterized by four spatial localizations of nitrogen atoms belonging to the groups in the projection of the structure on the *XZ* plane (denoted by the numbers 1–4). It has been found [49] that ferroelectric ordering of DMA groups between 1–2 position axis is accompanied by the antiferroelectric one along the 3–4 axis and vice versa. It is expected that the similar nature of the ordering processes would be observed also

for $DMAAl_{1-x}Cr_xS$ crystals. It is quite likely here that similarly to the case of $[(CH_3)_2NH_2]Mn(HCOO)_3$ MOF the balance between superexchange and elastic energy leads to local distortion that modifies the hydrogen bond and DMA groups ordering and consequently the ferroelectricity. Compared with the conventional magnetostriction effect in long-range magnetic ordering phase, this local magnetoelastic interaction in the paramagnetic state would be much weaker, thus requiring high magnetic fields to amplify it.

With Cr content increase the overall sample deformation goes via critical point modifying local magnetism and polarization. This assumption seems to be in agreement with the sensitive ferroelastic structure. This issue, however, deserves a further study including optimal Cr content determination. Nevertheless, some conclusions would be made on the basis of our experiment. One can suggest that the local deformation of the lattice affect ordering of both types of DMA group responsible respectively for the ferroelectric and antiferroelectric ordering. In both cases there arise the additional local polarizations of a different sign that compete with each other. The sum of these polarizations would nonlinearly depend on Cr content that manifests itself in the corresponding nontrivial changes of the spontaneous polarization (Fig. 3(a)) and the temperature of phase transition (Table 1). Such an approach also explains the different sign of the magnetoelectric coefficients in the two investigated compounds. Moreover, one can also explain nonfulfilment of inequality (5) for $DMAAl_{0.8}Cr_{0.2}S$ by more considerable contribution of the piezoelectric effect into the free energy (2) in comparison with the compound with a lower chromium concentration.

In conclusion, this study detailed on the ME coupling created in the initially diamagnetic DMAAS crystal by isomorphous substitution of Cr ion. The larger ME coupling for the sample with larger Cr content agrees well qualitatively within the simplified thermodynamic Landau analysis in the vicinity of ferroelectric transition. However, quantitative estimation implies other contributions as well. The observed nontrivial magnetic field dependence of ferroelectric transition can be explained within the model that takes into account influence of the arising local deformation of the lattice on the two types of DMA group responsible respectively for the ferroelectric and antiferroelectric ordering. Such a study should help in ME coupling ingenerating in similar compounds among the rich hybrid family of organic-inorganic compounds where ME interactions can be expected to exist closer to room temperature.

Acknowledgments

The authors express their gratitude to Prof. Z. Czapla from University of Wroclaw (Poland) for the offered samples and to Dr. B. Kundys from Institute de Physique et de Chemie des Matériaux de Strasbourg (France) for help in the magnetic measurements and fruitful discussion.

1. M. Fiebig, *J. Phys. Appl. Phys.* **38**, R123 (2005).
2. S.-W. Cheong and M. Mostovoy, *Nat. Mater.* **6**, 13 (2007).
3. M. Bibes and A. Barthélémy, *Nat. Mater.* **7**, 425 (2008).
4. C. Binek and B. Doudin, *J. Phys. Condens. Matter* **17**, L39 (2005).
5. L. Bogani and W. Wernsdorfer, *Nat. Mater.* **7**, 179 (2008).
6. M. Cinchetti, V.A. Dediu, and L.E. Hueso, *Nat. Mater.* **16**, 507 (2017).
7. D. Di Sante, A. Stroppa, P. Jain, and S. Picozzi, *J. Am. Chem. Soc.* **135**, 18126 (2013).
8. B. Kundys, A. Lappas, M. Viret, V. Kapustianyk, V. Rudyk, S. Semak, Ch. Simon, and I. Bakaimi, *Phys. Rev. B* **81**, 224434 (2010).
9. Bo Huang, Bao-Ying Wang, Zi-Yi Du, Wei Xue, Wei-Jian Xu, Yu-Jun Su, Wei-Xiong Zhang, Ming-Hua Zengc, and Xiao-Ming Chen, *J. Mater. Chem. C* **4**, 8704 (2016).
10. N.A. Hill, *J. Phys. Chem. B* **104**, 6694 (2000).
11. Y. Tokura and N. Kida, *Philos. Trans. R. Soc. Lond. Math. Phys. Eng. Sci.* **369**, 3679 (2011).
12. W. Eerenstein, N.D. Mathur, and J.F. Scott, *Nature* **442**, 759 (2006).
13. K. Singh, B. Kundys, M. Poienar, and C. Simon, *J. Phys. Condens. Matter* **22**, 445901 (2010).
14. W. Wang, L. Yan, J. Cong, Y. Zhao, F. Wang, S. Shen, T. Zou, D. Zhang, S. Wang, X. Han, and Y. Sun, *Sci. Rep.* **3**, 2024 (2013).
15. P. Jain, V. Ramachandran, R.J. Clark, H.D. Zhou, B.H. Toby, N.S. Dalal, H.W. Kroto, and A.K. Cheetham, *J. Am. Chem. Soc.* **131**, 13625 (2009).
16. H. Cui, Z. Wang, K. Takahashi, Y. Okano, H. Kobayashi, and A. Kobayashi, *J. Am. Chem. Soc.* **128**, 15074 (2006).
17. L.C. Gómez-Aguirre, B. Pato-Doldán, J. Mira, S. Castro-García, M.A. Señarís-Rodríguez, M. Sánchez-Andújar, J. Singleton, and V.S. Zapf, *J. Am. Chem. Soc.* **138**, 1122 (2016).
18. P. Li, W. Liao, Y. Tang, H. Ye, and Y. Xiong, *J. Am. Chem. Soc.* **139**, 8752 (2017).
19. Y. Tian, A. Stroppa, Y. Chai, L. Yan, Sh. Wang, P. Barone, S. Picozzi, and Y. Sunet, *Sci. Rep.* **4**, 6062 (2014).
20. D.-W. Fu, W. Zhang, H.-L. Cai, Yi Zhang, J.-Z. Ge, R.-G. Xiong, S.D. Huang, and T. Nakamura, *Angew. Chem. Int. Ed.* **50**, 11947 (2011).
21. R. Ramesh, *Nature* **461**, 1218 (2009).
22. W. Li, Zh. Wang, F. Deschler, S. Gao, R.H. Friend, and A.K. Cheetham, *Nat. Rev. Mater.* **2**, 201699 (2017).
23. B. Saparov and D.B. Mitzi, *Chem. Rev.* **116**, 4558 (2016).
24. W. Zhang and R.-G. Xiong, *Chem. Rev.* **112**, 1163 (2012).
25. W.-J. Xu, P.-F. Li, Y.-Y. Tang, W.-X. Zhang, R.-G. Xiong, and X.-M. Chen, *J. Am. Chem. Soc.* **139**, 6369 (2017).
26. M. Mon, J. Ferrando-Soria, M. Verdaguer, C. Train, Ch. Paillard, B. Dkhil, C. Versace, R. Bruno, D. Armentano, and E. Pardo, *J. Am. Chem. Soc.* **139**, 8098 (2017).
27. W.-Y. Zhang, Y.-Y. Tang, P.-F. Li, P.-P. Shi, W.-Q. Liao, D.-W. Fu, H.-Y. Ye, Y. Zhang, and R.-G. Xiong, *J. Am. Chem. Soc.* **139**, 10897 (2017).

28. D.-W. Fu, W. Zhang, H.-L. Cai, J.-Zh. Ge, Y. Zhang, and R.-G. Xiong*et*, *Adv. Mater.* **23**, 5658 (2011).
29. Da-Wei Fu, Wen Zhang, Hong-Ling Cai, Yi Zhang, Jia-Zhen Ge, Ren-Gen Xiong, Songping D. Huang, and Takayoshi Nakamura, *J. Am. Chem. Soc.* **133**, 12780 (2011).
30. D.-W. Fu, W. Zhang, H.-L. Cai, Y. Zhang, J.-Zh. Ge, R.-G. Xiong, and S.D. Huang, *Phys. Rev. Lett.* **110**, 257601 (2013).
31. D.-W. Fu1, H.-L. Cai1, Y. Liu, Q. Ye, W. Zhang, Y. Zhang, X.-Y. Chen, G. Giovannetti, M. Capone, J. Li, and R.-G. Xiong, *Science* **339**, 425 (2013).
32. W.-Y. Zhang, Q. Ye, D.-W. Fu, and R.-G. Xiong, *Adv. Funct. Mater.* **27**, 1603945 (2017).
33. L.F. Kirpichnikova, L.A. Shuvalov, N.R. Ivanov, B.N. Prasolov, and E.F. Andreyev, *Ferroelectrics* **96**, 313 (1989).
34. V. Kapustianik, M. Fally, H. Kabelka, and H. Warhanek, *J. Phys. Condens. Matter* **9**, 723 (1997).
35. G. Völkel, N. Alsabbagh, R. Böttcher, D. Michel, B. Milsch, Z. Czapla, and J. Furtak, *J. Phys. Condens. Matter* **12**, 4553 (2000).
36. V. Kapustianik, Z. Czapla, R. Tchukvinskyi, A. Batiuk, Yu. Eliyachevskyy, Yu. Korchak, and V. Rudyk, *Phys. Status Solidi A* **201**, 139 (2004).
37. V. Kapustianyk, Yu. Eliyashevskyy, Z. Czapla, S. Dacko, O. Czupi, V. Rudyk, R. Serkiz, S. Sereda, and S. Semak, *Acta Phys. Pol. A* **127**, 791 (2015).
38. V. Kapustianyk, Yu. Eliyashevskyy, Z. Czapla, V. Rudyk, R. Serkiz, N. Ostapenko (Loboda), I. Hirnyk, J-F. Dayen, M. Bobnar, R. Gumeniuk, and B. Kundys, *Scientific Rep.* **7**, 14109 (2017).
39. V. Kapustianyk, Yu. Eliyashevskyy, Z. Czapla, S. Dacko, V. Rudyk, and N. Ostapenko, *Ferroelectrics* **510**, 80 (2017).
40. R.D. Shannon, *Acta Crystallogr. A* **32**, 751 (1976).
41. W. Eerenstein, N.D. Mathur, and J.F. Scott, *Nature* **442**, 759 (2006).
42. H. Schmid, *Ferroelectrics* **161**, 1 (1994).
43. M.E. Lines, A.M. Glass, *Principles and Applications of Ferroelectrics and Related Materials*, Clarendon Press, Oxford (1977), p. 680.
44. T. Lottermoser, T. Lonkai, U. Amann, D. Hohlwein, J. Ihringer, and M. Fiebiget, *Nature* **430**, 541 (2004).
45. V. Kapustianyk, Yu. Eliyashevskyy, Z. Czapla, S. Dacko, V. Rudyk, S. Sereda, and N. Ostapenko, *Phase Transitions* **90**, 175 (2017).
46. S.L. Hou and N. Bloembergen, *Phys. Rev.* **138**, A1218 (1965).
47. B.K. Ponomarev, S.A. Ivanov, B.S. Red'kin, and V.N. Kurlov, *Physica B* **177**, 327 (1992).
48. R.I. Thomson, P. Jain, A.K. Cheetham, and M.A. Carpenter, *Phys. Rev. B* **86**, 214304 (2012).
49. I.V. Stasyuk and J.V. Velychko, *J. Phys. Stud.* **4**, 92 (2000).

Про магнітоелектричний ефект у парамагнітних кристалах $NH_2(CH_3)_2Al_{1-x}Cr_x(SO_4)_2{\cdot}6H_2O$

В. Капустяник, Н. Лобода, Ю. Еліяшевський, С. Семак

Представлено результати вивчення нещодавно виявленої можливості індукування і зміни знаку магнітоелектричної (ME) взаємодії у кристалах $NH_2(CH_3)_2Al_{1-x}Cr_x(SO_4)_2{\cdot}6H_2O$ у залежності від концентрації хрому. ME взаємодія, зокрема збільшення абсолютного значення ME коефіцієнта при збільшенні концентрації хрому, добре узгоджується на якісному рівні з термодинамічною теорією Ландау. Проте кількісна оцінка передбачає також врахування й інших внесків. Нетривіальну залежність температури сегнетоелектричного фазового переходу від прикладеного магнітного поля може бути пояснено у моделі, яка враховує вплив результуючої локальної деформації ґратки на два типи груп DMA, що відповідають за сегнетоелектричне та антисегнетоелектричне впорядкування.

Ключові слова: магнітоелектрична взаємодія, парамагнетик, сегнетоелектричний перехід.

О магнитоэлектрическом эффекте в парамагнитных кристаллах $NH_2(CH_3)_2Al_{1-x}Cr_x(SO_4)_2{\cdot}6H_2O$

В. Капустянык, Н. Лобода, Ю. Элияшевский, С. Семак

Представлены результаты изучения недавно обнаруженной возможности индуцирования и изменения знака магнитоэлектрического (МЭ) взаимодействия в кристаллах $NH_2(CH_3)_2Al_{1-x}Cr_x(SO_4)_2{\cdot}6H_2O$ в зависимости от концентрации хрома. МЭ взаимодействие, в частности увеличение абсолютного значения МЭ коэффициента при увеличении концентрации хрома, хорошо согласуется на качественном уровне с термодинамической теорией Ландау. Однако количественная оценка предполагает также учет и других вкладов. Нетривиальная зависимость температуры сегнетоэлектрического фазового перехода от приложенного магнитного поля может быть объяснена в модели, учитывающей влияние результирующей локальной деформации решетки на два типа групп DMA, отвечающих за сегнетоэлектрическое и антисегнетоэлектрическое упорядочение.

Ключевые слова: магнитоэлектрическое взаимодействие, парамагнетик, сегнетоэлектрический переход.